Salem, R.; Monteiro, R.; Gutierrez, CF.; Borrell Tomás, MA.; Salvador Moya, MD.; Chinelatto, AS.; Chinelatto, A.... (01-0). Effect of Al2O3-NbC nanopowder incorporation on the mechanical properties of 3Y-TZP/Al2O3-NbC nanocomposites obtained by conventional and spark plasma sintering. Ceramics International. 44(2):2504-2509. https://doi.org/10.1016/j.ceramint.2017.10.235

Effect of incorporate of Al_2O_3-NbC nanopowders on the mechanical properties of 3Y-TZP-Al_2O_3-NbC nanocomposites obtained by conventional and spark plasma sintering

R. E. P. Salem, F. R. Monteiro, C. F. Gutiérrez-González[2], A. Borrell[3], M. D. Salvador[3], A. S. A. Chinelatto, A. L. Chinelatto, E. M. J. A. Pallone[1]

[1]Universidade de São Paulo/Faculdade de Zootecnia e Engenharia de Alimentos; Av. Duque de Caxias Norte, 225, 13635-900 Pirassununga-SP, Brazil
[2]Centro de Investigación en Nanomateriales y Nanotecnología (Consejo Superior de Investigaciones Científicas, Universidad de Oviedo, Principado de Asturias), Avenida de la Vega 4-6, 33940 El Entrego, Spain
[3]Instituto de Tecnología de Materiales (ITM), Universitat Politècnica de València, Camino de Vera s/n, 46022 Valencia, Spain

Abstract

The effect of incorporation Al_2O_3-NbC nanopowders to reinforce 3Y-TZP matrix and the influence on mechanical properties of 3YTZP-Al_2O_3-NbC nanocomposites obtained by conventional and spark plasma sintering (SPS) was investigated. The nanometric powders of Al_2O_3-NbC were prepared by reactive high-energy milling, deagglomerated, leached with acid, and added to the 3Y-TZP matrix in the proportion of 5 vol%. The final powders were dried under airflow, compacted and sintered at the temperature range of 1300–1500 °C. The effect of sintering technique and final temperature on the microstructure and mechanical properties, such as hardness, toughness and Young's modulus were analyzed.
An important mechanical value obtained in all materials reinforced with Al_2O_3-NbC nanopowders is the fracture toughness, which differ significantly of the 3Y-TZP monolithic material (5.2 MPa·$m^{1/2}$). The nanocomposites sintered conventionally at 1450°C show the higher fracture toughness (8.7 MPa·$m^{1/2}$).
Microstructure observations indicate that NbC nanoparticles are dispersed homogeneously within 3Y-TZP matrix and limited their grain growth. However, the partial oxidation of the NbC in the surface of the nanocomposites found a limit in the conventional sintering temperature, since the samples sintered at 1500°C showed a reduction in fracture toughness.

Keywords:
Nanocomposite, Al_2O_3-NbC, 3Y-TZP, Spark plasma sintering, Mechanical properties, Microstructure.

1. Introduction

Recent research on zirconia-alumina composites has been showing advances on applications of these materials in engineering, especially in cutting tools, biomaterials and other applications that require high wear resistance [1-4].

The use of carbides of transition metals as a reinforcement on the ceramic matrix is one promising option, since the presence of these carbides enhances mechanical properties, such as hardness and fracture toughness, and improves tribological properties [5-7].

Niobium carbide (NbC) is one of the transition metallic carbides used to produce hard metals. It combines a high melting point with high hardness and low chemical reactivity [8,9]. The similar thermal expansion coefficients between NbC, Al_2O_3 and ZrO_2 allow composites of these materials to have a good performance, despite the variation of temperature, enhancing durability of parts and products which use this material [9,10].

Among the various synthesis methods for producing nanometric powders, the reactive milling is one interesting option, in which high-energy milling promotes a solid-state reaction in a mixture of reactive powders [10-13]. Some advantages of this method are the ability to reduce particle size to nanometer scale, good stoichiometry and low energetic cost [10,11]. However, the high temperatures reached in the reaction during milling can produce strong agglomeration of particles, making necessary further milling time to deagglomerate the powder after synthesis [10,12,13].

Several authors have reported the potential of the use of NbC as grain growth inhibitor in WC-Co hard metals [14], and as hardening reinforcing material in ZrO_2 and Al_2O_3 matrix [10,15,16]. This suggests that NbC as a reinforcing material deserves to be further investigated.

Alecrim et al. [10] studied Al_2O_3-5 vol% NbC composites by a preparation technique similar to the one used in this work. The composites sintered by SPS at 1450°C attained full density and homogeneous distribution of NbC particles in the alumina matrix, and with hardness of 25.4 GPa and fracture toughness of 2.9 $MPa \cdot m^{1/2}$.

Pallone et al. [12] obtained alumina matrix composites with 5 wt% of NbC synthesized by reactive milling and sintered by high vacuum in a conventional high temperature furnace (1450°C and 1500°C), attaining 96 and 98% of theoretical density and hardness values of 17 and 18 GPa, respectively. They showed that the inhibition of alumina grain growth, caused by the presence of NbC particles, was important to improve the mechanical properties.

Santos et al. [16] studied ZrO_2-NbC composites, obtained from commercial powders, by pressureless hot pressing at 1600°C without sintering additives. They found that the addition of NbC enhances the hardness of sintered samples and this fact can make possible the use of the composite in cutting tools. However, fracture toughness was sensitive to the combination of composition and sintering parameters, which is important to be analyzed.

Considering that yttria-stabilized tetragonal zirconia has a relatively good fracture toughness among other advanced monolithic ceramic materials [2,3], with addition of harder phases, such as alumina and niobium carbide, the utilization of this material for cutting tools, internal prostheses and other applications that require high wear resistance can be studied.

In the case of NbC, it has a very high melting point (3490°C) and a coefficient of thermal expansion close to that of 3Y-TZP ($6 – 9 \times 10^{-6}$ $°C^{-1}$ against $8 – 10.5 \times 10^{-6}$ $°C^{-1}$, respectively) [9,10], which helps to reduce internal stresses during the sintering process and applications that require variation of temperature.

In order to improve the sinterability of these materials and to obtain mechanical and wear properties with a higher quality than the current properties, spark plasma sintering (SPS) is known as an interesting technique, also known as field-assisted sintering technique (FAST). This technique can work at heating rates on the order of hundreds of degrees per minute, reaching high temperatures in very short time, providing dense materials after cycles of heating/cooling of only a few minutes. Furthermore, due to its promising properties, currently there is a growing interest in the sintering of oxide and non-oxide ceramic powders and hard metals by SPS [17,18].

Therefore, the aim of this work was to study the effect of incorporation of Al_2O_3-NbC nanopowders prepared via reactive milling in a 3Y-TZP matrix and sintered without additives using spark plasma sintering technique (SPS) and compared with conventional sintering. The microstructural characteristics, as well as, the mechanical properties of these 3YTZP-Al_2O_3-NbC nanocomposites were investigated and discussed in detail.

2. Experimental procedure

2.1. Preparation of the powder

The nanometric powders of alumina (Al_2O_3) and niobium carbide (NbC) were obtained by reactive high-energy milling as described in a previous work [12,19]. High-energy ball milling of the reactant powder mixtures of Al-Nb_2O_5-C-Al_2O_3 were carried out using commercial powders of aluminum (ALCOA, 99.7% of purity), Nb_2O_5 (CBMM, 98.5% of purity), Al_2O_3 (AKP-53, Sumitomo, 99.95% of purity) and carbon black.

The milling equipment used for this reaction was the Shaker Mix-type mill, SPEX 8000, with hardened steel vial and milling balls. The ball/material mass ratio was fixed in 5:1, using five balls with 11 mm in diameter. The ignition time of the reaction was 190 min (when the activation of the reaction occurred, with increase of external temperature of the vial) and the total time of the process was 330 min, to reduce the crystallite size to the nanometric scale. After synthesis, the powders were leached in hydrochloric acid for removal of iron contamination from the vial and grinding media, and deagglomerated in a planetary mill (Fritsch mill), as described in a previous work [20]. After this process, a semi-quantitative elemental analysis of the Al_2O_3-NbC powder by X-ray fluorescence spectroscopy (Shimadzu EDX-720, Japan) was performed in order to verify the amount of remaining impurities from the grinding media.

The incorporation of the Al_2O_3-NbC powder synthesized by the procedure described above was done in a volume fraction of 5% on a 3Y-TZP powder (TZ-3Y-E, Tosoh, Japan) by mixing alcoholic suspensions of both components by ball milling with zirconia 5 mm balls using pure HDPE flasks. The dispersant used for this mixture was 4-aminobenzoic acid (PABA), at 0.2 wt% of the total powder mass. Also, 0.5 wt% of oleic acid was added, in order to lubricate the composite powder for conformation.

2.2. Sintering process

Before the conventional sintering, the powders were dried, sieved until 80 μm and isostatically pressed at 200 MPa in the shape of 20 mm cyllinders. Conventional sintering was carried out in a high-temperature furnace at the temperatures of 1400, 1450 and 1500°C, with a heating rate of 10°C/min and a dwell time of 120 min. A dwell time of 60 min at 600°C was also done to eliminate the organic material. To prevent the inherent oxidation of NbC in

oxidizing atmospheres and to promote a reductive atmosphere into the furnace, which did not have control of atmosphere, the samples were put into graphite powder in an alumina crucible, prior to sintering.

A second set of powders was introduced into a 20-mm diameter graphite die and sintered using a spark plasma sintering (SPS) apparatus (HP D25/1, FCT Systeme GmbH, Germany), at the temperatures of 1300, 1350 and 1400°C and pressure applied of 80 MPa, to obtain fully sintered bulk materials. The tests were carried out under vacuum at a heating rate of 100ºC/min with 5 min of dwelling time at the maximum temperature. For comparison with the nanocomposites, a set of 3Y-TZP samples without any addition, sintered conventionally at 1550ºC for 2 h, were also analyzed by the means of mechanical and microstructural properties.

2.3. Characterization

Phase composition of the powder after reaction was characterized by X-ray diffraction (XRD, Rigaku diffractometer, MiniFlex 600 model). The measurements were taken in the 10-90º range and the step size and time of reading were 0.02º and 0.3 s, respectively. With this diffraction pattern, the refinement of structural parameters by the Rietveld method was made, to quantify the phases of Al_2O_3 and NbC. The crystallite size was determined using the width of the Bragg peak profiles at half of the maximum intensity, according to Scherrer method [19].

The density of the samples was measured by the Archimedes' principle (ASTM C373-88). Relative densities were estimated in accordance with the theoretical density of the composite, calculated by mixture rule (6.03 g/cm^3).

For microstructural characterization, the sintered samples were fractured on their cross-section and polished with SiC paper and diamond particle suspensions. The fracture surface was analyzed by using a field emission gun scanning electron microscope (FE-SEM, HITACHI S-4800, SCSIE, Valencia University).

Young's modulus (E) of the composites were determined by nanoindentation technique (Model G200, MTS Company, USA). Tests were performed under maximum depth control (2000 nm), using a Berkovich

diamond tip previously calibrated on fused silica standard. The contact stiffness was determined by the Continuous Stiffness Measurement (CSM) technique, to calculate the elastic modulus [20]. Amplitude was programmed to 2 nm with frequency of 45 Hz. A matrix of 25 indentations was made on each sample, to determine the average modulus. The Poisson's coefficient was 0.3 for all calculations considering a fully dense material.

Mechanical properties were evaluated via macro and micro-indentation techniques. The hardness of the composites was determined by Vickers microindentation, with a load of 1 kgf for 12 s, in a Shimadzu HMV equipment. Ten indentations were made in each sample. K_{IC} values were studied by the cracks induced by applying loads of 20 kg for 10 s in a regular durometer with a Vickers diamond tip. The crack lengths and half-diagonals of the indentations were measured using an image analysis program, and fracture toughness was calculated by the equation proposed by Niihara et al. [21].

3. Results and discussion

3.1. Powder characterization

Figure 1 shows the X-ray diffractograms (XRD) of the reactants and the products of the reaction performed by high-energy ball milling. While the first diffractogram shows peaks of all phases of the reactants (Al, C, Nb_2O_5 and Al_2O_3 as diluent), the XRD pattern for the product shows only peaks of the reaction products (Al_2O_3 and cubic NbC). The calculated crystallite size of the present phases was and 37.0 and 19.5 nm for Al_2O_3 and NbC, respectively.

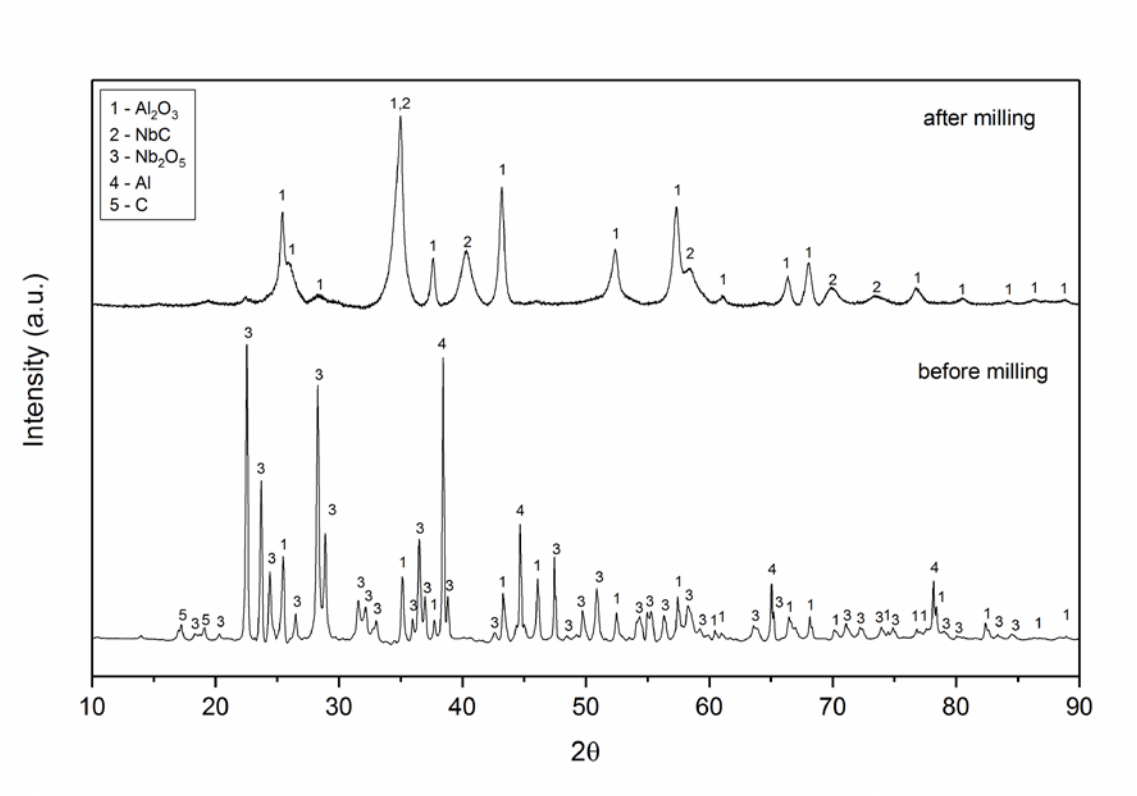

Figure 1 – XRD of precursor powders (a) before high-energy milling; (b) after high-energy milling.

The high temperatures during high-energy ball milling caused a large agglomeration of the particles produced by the reaction inside the mill. The hard aggregates produced were submitted to a new milling process, in a planetary mill, to break the powder agglomerates to a nanocrystalline scale.

Figure 2 shows transmission micrograph of the Al_2O_3-NbC powder after deagglomeration in a planetary mill. The powder is mostly in the form of submicrometric aggregates of nanometric Al_2O_3 and NbC particles (dark and clear particles, respectively). The primary particle size is similar to the one calculated by Scherrer's method, although there can be found smaller particles as well.

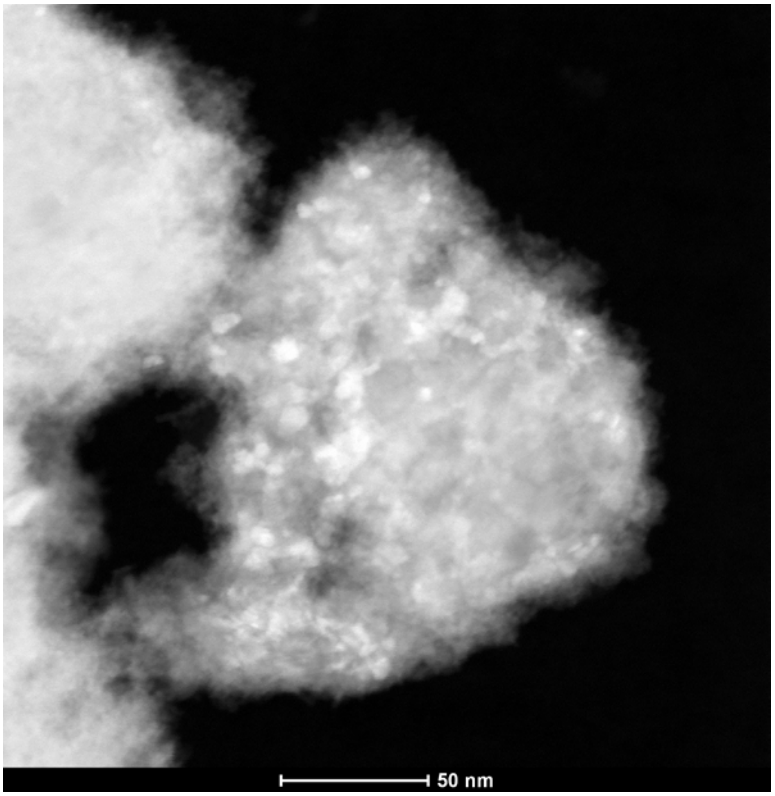

Figure 2 – TEM of an Al_2O_3-NbC powder aggregate after planetary milling.

3.2 Characterization of ZrO_2/5 vol% (Al_2O_3-NbC) nanocomposites obtained by conventional sintering and SPS

Table 1 shows the relative density values (% TD) and mechanical properties, H_v, E and K_{IC} values, for all nanocomposites sintered in the temperature range of 1300-1500ºC. It is noted that all the temperatures in which the powders were sintered allowed obtaining materials with relatively high density, although not with full density. The density in the nanocomposites sintered by SPS is higher than the ones sintered conventionally.

Regarding hardness properties, H_v values, the samples sintered by SPS at 1350 ºC show values similar to those obtained for conventional at 1500 ºC. This is an important result, because temperature is 150 ºC less and, also, the saving time and energy by SPS is significant. These aspects are ones of the main criteria for the selection of the material for cutting tool application [22.23].

About the elastic modulus values, those were high in the nanocomposites sintered by conventional and SPS.

Nevertheless, the highest fracture toughness was found in the nanocomposites sintered conventionally at 1450 °C, with a significant reduction, down to 6.5±0.3 $MPa \cdot m^{1/2}$, in the nanocomposites sintered at 1500 °C. This reduction can be explained by a partial oxidation and consequent expansion of the NbC present in the reinforcement. Although the temperature range for oxidation of pure stoichiometric NbC is 500-600 °C [24], the volumetric expansion coefficient of NbC rises significantly with temperature, as showed by Ajami et al. [25]. Connoley et al. [26] estimated that the maximum volume expansion factor for the transformation of NbC to Nb_2O_5 is 2.28, based on crystallographic data. Also, based on the study of Sjoberg et al. [27], the volume expansion of oxidizing primary carbides was identified as a mechanism of environmentally assisted crack propagation, due to the stress intensifying effect of expanding particles at or near crack tips. Therefore, the partial releasing of niobium onto grain boundaries, seems to have formed an embrittling Nb_2O_5 phase, starting from the surface of the nanocomposite specimen [28]. However, it is important to note that the 3Y-TZP matrix and the graphite powder used in the conventional sintering without atmosphere control were somewhat effective to retard the oxidation of NbC and prevent it under 1500 °C, allowing to keep the NbC structure by means of a simple operation arrangement, though only up to a certain limit.

Regarding fracture toughness of samples, the best value obtained corresponds to sample sintered at 1400 and 1450 ºC by conventional. Presenda et al. [29] sintered 3Y-TZP material by conventional at 1400 ºC with 2 h of holding time and found fracture toughness values around 6.4 $MPa \cdot m^{1/2}$. Therefore, these results are 20% higher that those found in other studies under similar conditions.

Table 1 – Properties of the ZrO_2/5 vol% (Al_2O_3-NbC) nanocomposites obtained by conventional sintering and SPS.

Properties	SPS sintering temperatures (°C)			Conventional sintering temperatures (°C)		
	1300	1350	1400	1400	1450	1500
Density (%TD)	98.5	98.1	98.7	95.8	97.4	97.5
Hardness (GPa)	11.3±0.4	12.7±0.2	12.1±0.6	9.8±0.3	10.8±0.3	13.2±0.3

Young's Modulus (GPa)	237±3	240±3	234±4	219±9	225±3	230±4
Toughness ($MPa \cdot m^{1/2}$)	6.3±1.0	7.2±1.4	8.1±1.9	8.1±1.1	8.7±1.2	6.5±0.3

Figure 3 shows the microstructure of all the sintered nanocomposites, in which there can be seen a small amount of porosity present in the samples. In all micrographs, there can be seen very small NbC particles (white spots) embedded into the microstructure of the 3Y-TZP matrix. The microstructure is very narrow and dense, with mixed inter- and intragranular fracture of the grains. There can be seen a difference in the fracture mode between the sintering methods. The nanocomposites sintered conventionally show a mixed fracture mode (inter- and transgranular fracture), while SPS-sintered nanocomposites show predominantly intergranular fracture, although some regions of transgranular fracture can also be observed. Comparing the microstructure based on the temperatures in the same sintering technique, there was not a significant variation in the microstructure with sintering temperature.

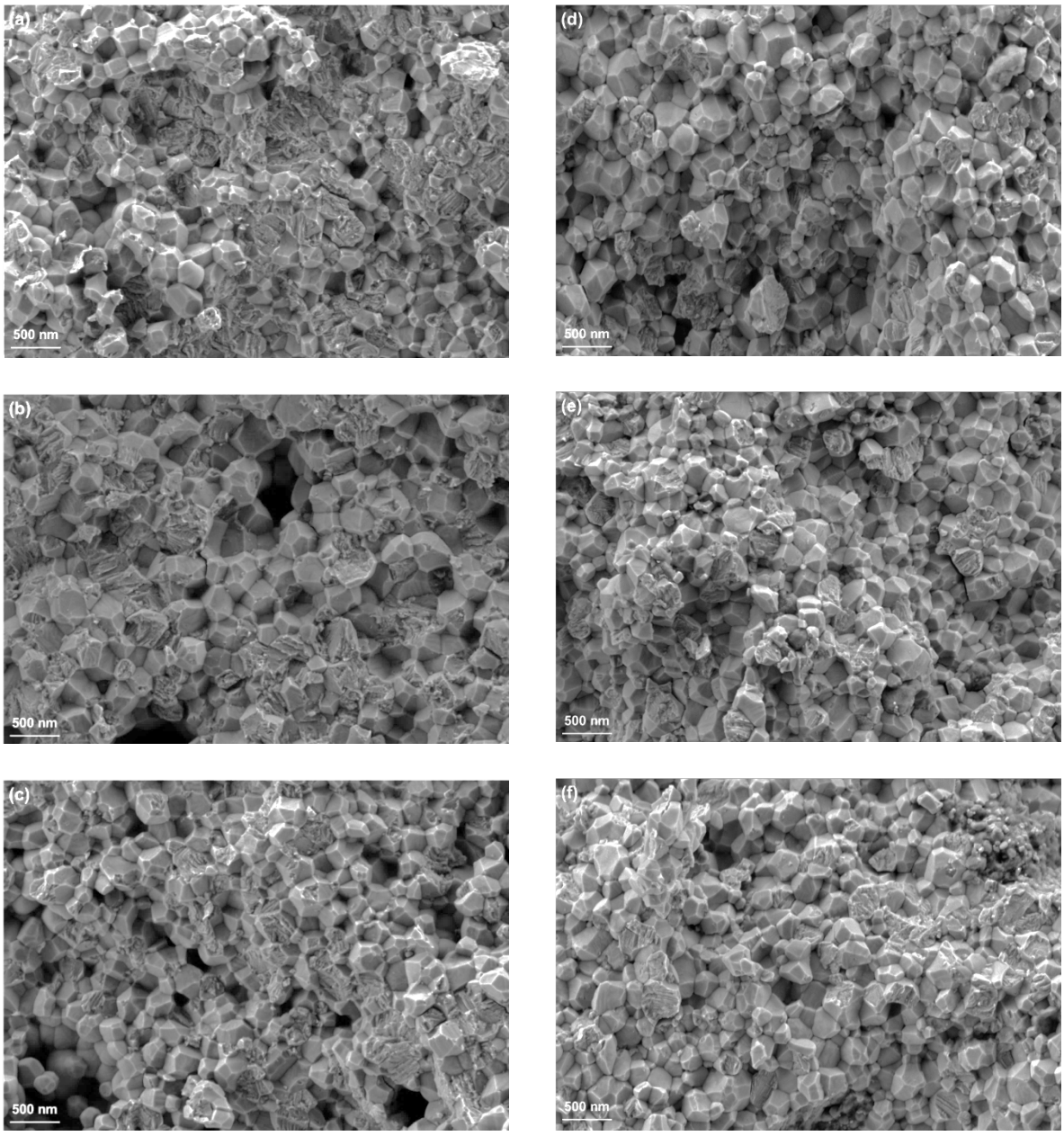

Figure 3 – SEM micrographs of the fracture surface of the 3Y-TZP/5 vol% (Al_2O_3-NbC) nanocomposites by conventional sintering at: 1400ºC (a), 1450°C (b), 1500°C (c); and by SPS at: 1300°C (d); 1350°C (e), 1400°C (f).

The microstructure of SPS nanocomposites is very similar to the microstructure of the nanocomposites sintered conventionally. There can be seen small NbC particles and small agglomerates dispersed in the microstructure, with approximate mean particle diameter of 50 nm. The mean grain size of the matrix does not exceed 400 nm, and there was no significant

difference on the grain size between the sintering temperatures studied. Pullout of the NbC particles can be observed at some grain corners. As expected, the temperature and time needed to achieve a dense and narrow microstructure by the SPS technique was as low as 1300°C/5 min, although 1400°C/5 min was the sintering condition that showed the best combination of properties; the uniaxial pressure applied during the process plays an important role on the rapid consolidation of the microstructure, making this technique very suitable for the production of this nanocomposite.

Figure 4 shows the microstructure of 3Y-TZP, sintered conventionally and by SPS at 1400ºC, in the same condition used for the 3Y-TZP/5 vol% (Al_2O_3-NbC) nanocomposites.

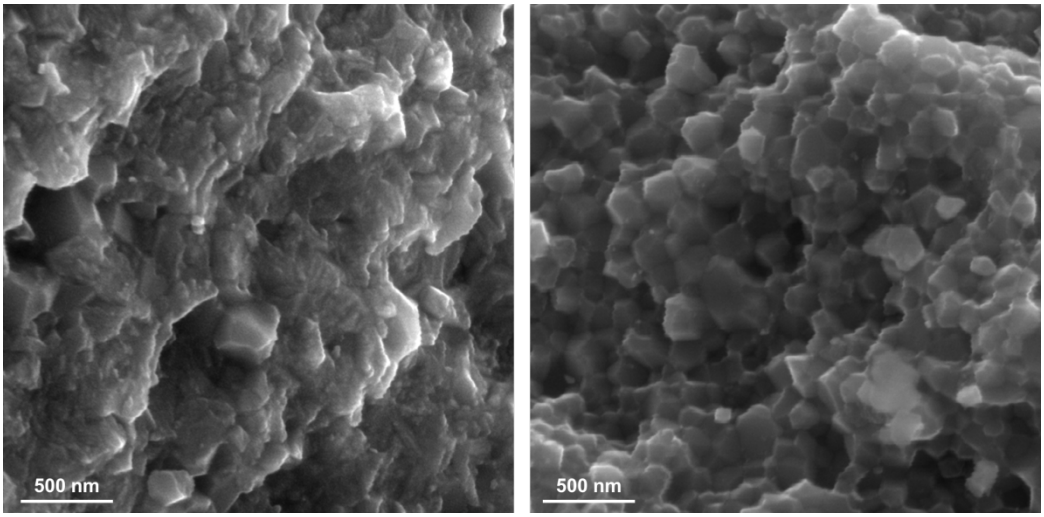

Figure 4 – SEM micrograph of fracture surface of 3Y-TZP: (a) sintered conventionally at 1400°C/2 h and (b) by SPS at 1400°C/5 min.

Comparing the nanocomposites with samples of 3Y-TZP, sintered at 1400°C (Figure 4), there can be seen that the Al_2O_3-NbC nanoparticles reinforcement helped to increase both Young's modulus and fracture toughness (210 GPa and 5.2 MPa·$m^{1/2}$, respectively, for 3Y-TZP sintered conventionally, although a reduction in the hardness was identified for the conventional sintering at 1400°C and 1450°C. The higher Young's modulus and fracture toughness can be related to the crack deviation caused by the presence of the

nanoparticles in grain boundaries, as proposed by various authors [30-31]. On the other hand, the reduction in the hardness for some conditions is related to the porosity present in the microstructure [32-33]

Fig. 4 also shows a different fracture mode with the sintering technique, being predominantly transgranular in the 3Y-TZP sintered conventionally and intergranular in the one sintered by SPS.

The difference on the fracture toughness is mostly related with the fracture mode. However, the role of the grain size itself on the fracture toughness and energy is not quite clear in the literature. Winnubst et al. [34], showed that the length of a crack through a material is for intergranular cracks about two times larger than for transgranular cracks, independent of the grain size. Also, literature shows many cases in which a small amount of reinforcement can be influenced by fine control of micro/nanostructure of the material and changed the fracture mode, mechanical and electrical properties [34-36]. According to Acchar and Segadães [15], transgranular fracture can contribute to increasing flexural strength of the matrix, while intergranular fracture is related to the high interface fracture energy and the crack deflection mechanism, promoting an increase in the fracture toughness of the matrix.

Therefore, considering that the grain size did not vary significantly with the sintering technique and/or temperature, the amount of porosity, which is directly related to sintered final density, was the factor that most influenced on the hardness of the nanocomposites. On the other hand, Young's modulus and fracture toughness were influenced by the fracture mode. The improvement observed in mechanical properties can be mostly attributed to the microstructural change induced by the presence of the Al_2O_3-NbC nanoparticles and to the crack deflection mechanism. The first effect changes the grain boundary region and alters the relation of plastic deformation of the matrix during the Vickers indentation, while deflection mechanisms promote an enhancement in the fracture toughness.

The introduction of 5 vol% Al_2O_3-NbC nanoparticles in the 3Y-TZP matrix showed a significant improvement on Young's modulus and fracture toughness for both conventional and spark plasma sintering techniques. The best results were found for the nanocomposites sintered at 1400°C by SPS and 1450°C by conventional sintering with graphite powder protection. Based on these results,

there can be suggested a “processing window” for this specific nanocomposite, a range of temperatures that allow the production of nanocomposites with improved mechanical strength, with potential use on applications that require high wear resistance and durability, also considering the limitation of the process caused by potential oxidation of NbC particles during conventional sintering in an environment not totally free of oxygen.

4. Conclusions

3Y-TZP reinforced with 5 vol% Al_2O_3-NbC nanopowders were successfully produced both by conventional and spark plasma sintering. The narrow microstructure allowed to achieve high density. The hardness was sensively influenced by porosity, and fracture toughness was higher in all nanocomposites. Spark plasma sintering allowed to obtain nanocomposites with microstructure similar to conventional sintering, in a much shorter time. Comparing with 3Y-TZP, the change in the fracture mode played an important role in the crack deflection, strongly influencing fracture toughness, especially in the samples sintered conventionally. However, the partial oxidation of NbC was observed for the highest conventional sintering temperature (1500°C), reducing fracture toughness of the nanocomposite for this sintering condition, and this limitation must be taken in account. Based on these promising results, there can be suggested a “processing window” for this composition, a range of temperatures that allow the production of these nanocomposites with improved mechanical properties.

Acknowledgements

The authors acknowledge the Brazilian institution CAPES-PVE (project 23038.009604/2013-12) and FAPESP (project 2015/07319-8); European Union/Erasmus Mundus for doctorate mobility supported; Spanish Ministry of Economy and Competitiveness (IJCI-2014-19839).

References

[1] A.H. De Aza, J. Chevalier, G. Fantozzi, M. Schehl, R. Torrecillas, Crack growth resistance of alumina, zirconia and zirconia toughened alumina ceramics for joint prostheses, Biomaterials 23 (2002) 937-945.

[2] A. Senthil, Kumar, A. Raja Durai, T. Sornakumar, Development of alumina-ceria ceramic composite cutting tool, Int. J. Refract. Met. Hard Mater. 22 (2004) 17-20.
[3] F. Zhang, J. Chevalier, C. Olagnon, B.V. Meerbeek, J. Vleugels, slow crack growth and hydrotermal aging stability of an alumina-toughened zirconia composite made from La_2O_3-doped 2Y-TZP, J. Eur. Ceram. Soc. 37 (2017) 1865-1871.
[4] R. Benavente, M.D. Salvador, F.L. Penaranda-Foix, E. Pallone, A. Borrell, Mechanical properties and microstructural evolution of alumina–zirconia nanocomposites by microwave sintering, Ceram. Int. 40 (2014) 11291-11297.
[5] L.R.R. Alecrim, J.A. Ferreira, C.F. Gutiérrez-González, M.D. Salvador, A. Borrell, E.M.J.A. Pallone, Sliding wear behavior of Al_2O_3-NbC composites obtained by conventional and nonconventional techniques, Tribol. Int. 110 (2017) 216-221.
[6] W. Acchar, C.R.F. Camara, C.A.A. Cairo, M. Filgueira, Mechanical performance of alumina reinforced with NbC, TiC and WC, Mater. Res. 15 (2012) 821-824.
[7] X.H. Zhang, C.X. Liu, M.S. Li, J.H. Zhang, J.L. Sun, Toughening mechanism of alumina-matrix ceramic composites with the addition of AlTiC master alloys and ZrO_2, Ceram. Int. 35 (2009) 93-97.
[8] H.O.H. Pierson, Handbook of Refractory Carbides & Nitrides: properties, characteristics, processing and apps. Noyes Publications, New Jersey, 1996.
[9] C.P. Kempter, E.K. Storms, Thermal expansion of some niobium carbides, J. Less Comm. Met. 13 (1967) 443-447.
[10] L.R.R. Alecrim, J.A. Ferreira, C.F. Gutiérrez-González, M.D. Salvador, A. Borrell, E.M.J.A. Pallone, Effect of reinforcement NbC phase on the mechanical properties of Al_2O_3-NbC nanocomposites obtained by spark plasma sintering, Int. J. Refract. Met. Hard Mater. 64 (2017) 255-260.
[11] L. Takacs, Reduction of magnetite by aluminum: a displacement reaction induced by mechanical alloying, Mater. Lett. 13 (1992) 119-124.
[12] E.M.J.A. Pallone, V. Trombini, W.J. Botta, R. Tomasi, Synthesis of Al_2O_3-NbC by reactive milling and production of nanocomposites, J. Mater. Proc. Tech. 143-144 (2003) 185-190.
[13] C. Suryanarayana, Nanocrystalline materials, Int. Mater. Rev. 40 (1995) 41-64.
[14] S.G. Huang, R.L. Liu, L. Li, O. Van der Biest, J. Vleugels, NbC as a grain growth inhibitor and carbide in WC-Co hard metals, Int. J. Refract. Met. Hard Mater. 26 (5) (2008) 389-395.
[15] W. Acchar, A.M. Segadães, Properties of sintered alumina reinforced with niobium carbide, Int. J. Refract. Met. Hard Mater. 27 (2009) 427-430.
[16] C. Santos, L.D. Maeda, C.A.A. Cairo, W. Acchar, Mechanical properties of hot pressed ZrO_2-NbC ceramic composites, Int. J. Refract. Met. Hard Mater. 26 (2008) 14-18.
[17] A. Borrell, A. Fernandez, R. Torrecillas, J.M. Cordoba, M.A. Aviles, F.J. Gotor, Spark plasma sintering of ultrafine TiC_xN_{1-x} powders synthesized by a mechanically induced self-sustaining reaction, J. Am. Ceram. Soc., 93 (8) (2010) 2252-2256.
[18] V. Bonache, M.D. Salvador, A. Fernandez, A. Borrell, Fabrication of full density near-nanostructured cemented carbides by combination of VC/Cr_3C_2

addition and consolidation by SPS and HIP Technologies, Int. J. Refract. Met. Hard Mater. 29 (2011) 202-208.
[19] H. Klung, L. Alexander, X-ray Diffraction Procedures, Wiley, New York, 1962.
[20] W.C. Oliver, G.M. Pharr, An improved technique for determining hardness and elastic modulus using load and displacement sensing indentation experiments, J. Mater. Res. 7 (1992) 1564-1583.
[21] K. Niihara, R. Morena, D.P.H. Hasselman, Evaluation of K_{IC} of brittle solids by th indentation method with low crack-to-indentation ratios. J. Mater. Sci. Lett. 1 (1982) 13-16.
[22] F.W.J. Botta Filho, R. Tomasi, E.M.J.A. Pallone, A.R. Yavari, Nanostrucutured composites obtained by reactive milling, Scr. Mater. 44 (2001) 1735-1740.
[23] A.S.A. Chinelatto, E.M.J.A. Pallone, V. Trombini, R. Tomasi, Influence of heating curve on the sintering of alumina subjected to high-energy milling, Ceram. Int. 34 (2008) 2121–2127.
[24] M.G.V. Cuppari, S.F. Santos, Physical properties of the NbC carbide. Metals 6 (2016) 250-266.
[25] F. Ajami, R. MacCrone, Thermal expansion, Debye temperature and Gruneisen constant of carbides and nitrides. J. Less Common Met. 38 (1974) 101-110.
[26] T. Connolley, M.J. Starink, P.A.S. Reed, Effect on oxidation on high temperature fatigue crack initiation and short crack growth in Inconel 718. Proc. Superalloys 2000, TMS (2000), 435-444.
[27] G. Sjoberg, N-G. Ingesten, R.G. Carlson, Grain boundary δ phase morphologies, carbides and notch rupture sensitivity of cast alloy 718. Proc. 2nd Int. Symp. Superalloy 718, 625 & Various Derivatives, TMS (1991) 603-620.
[28] M. Gao, D.J. Dwyer, R.P. Wei, Niobium enrichment and environmental enhancement of creep crack growth in nickel-base superalloys. Scr. Metall. & Mater. 32 (1995) 1169-1174.
[29] A. Presenda, M.D. Salvador, F.L. Peñaranda-Foix, R. Moreno, A. Borrell, Effect of microwave sintering on microstructure and mechanical properties in Y-TZP materials used for dental applications. Ceram. Int. 41 (2015) 7125-7132.
[30] M.A. Meyers, A. Mishra, D.J. Benson, Mechanical properties of nanocrystalline materials. Progress Mat. Sci., 51 (2006) 427-556.
[31] H. Awaji, S.M. Choi, E. Yagi, Mechanisms of toughening and strengthening in ceramic-based nanocomposites. Mech. Mater. 34 (2002) 411-422.
[32] H.Y. Suzuki, K. Shinozaki, H. Kuroki, S. Tashima, Sintered microstructure and mechanical properties of high purity alumina ceramics made by high-speed centrifugal compaction process, Key Eng. Mater. 159-160 (1999) 187-192.
[33] A. Nevarez-Rascon, A. Aguilar-Elguezabal, E. Orrantia, M.H. Bocanegra-Bernal, On the wide range of mechanical properties of ZTA and ATZ based dental composites by varying the Al_2O_3 and ZrO_2 content. Int. J. Refract. Met. Hard Mater. 27 (2009) 962-970.
[34] A.J.A. Winnubst, K. Keizer, A. J. Burgraaf, Mechanical properties and fracture behaviour of ZrO_2-Y_2O_3 ceramics, J. Mat. Sci. 18 (1983) 1958-1966.
[35] A. Borrell, I. Álvarez, R. Torrecillas, V.G. Rocha, A. Fernández, Microstructural design for mechanical and electrical properties of spark plasma sintered Al_2O_3–SiC nanocomposites, Materials Science and Engineering A 534 (2012) 693– 698.

[36] K. Tajima, H.J. Hwang, M. Sando, K. Niihara, PZT nanocomposites reinforced by small amount of oxides. J. Eur. Ceram. Soc. 19 (1999) 1179-1182.